Supporting Information for

Multiplexed Imaging of Nanoparticles in Tissues using Laser Desorption/Ionization Mass Spectrometry

Bo Yan[1], Sung Tae Kim[1], Chang Soo Kim[1], Krishnendu Saha[1], Daniel F. Moyano[1], Yuqing Xing[1], Ying Jiang[1], Amy L. Roberts[2], Felix S. Alfonso[1], Vincent M. Rotello[1]* and Richard W. Vachet[1]*

[1]Department of Chemistry, University of Massachusetts, Amherst, MA 01003, USA

[2]Department of Veterinary and Animal Sciences, University of Massachusetts, Amherst, MA 01003, USA

* Corresponding authors:

Richard W. Vachet

Email: rwvachet@chem.umass.edu

Phone: (+1) 413-545-2733

Fax: (+1) 413-545-4490

Vincent M. Rotello

Email: rotello@chem.umass.edu

Phone: (+1) 413-545-2058

Fax: (+1) 413-545-4490

EXPERIMENTAL SECTION

Intravenous administration of gold NPs and collection of samples. 50 μL of each AuNP (2 μM) or AuNP mixture (concentration of each AuNP: 2 μM) was administrated intravenously to Balb/c mice. After 24 h, the mice were humanely sacrificed by the inhalation of carbon dioxide and cervical dislocation. Then, the organ samples were harvested for analysis. Each organ was cut into two parts. One half was used for ICP-MS analysis to determine total gold amount, and the other half for LDI-MS imaging.

LDI-MS imaging tissue preparation. Leica cryostats (CM 3050 or 1850) were used to slice tissue. Tissues were sliced to 12 μm under -20 °C, and attached to indium tin oxide (ITO) coated glass slides.

LDI-MS instrumentation and conditions. LDI-MS imaging was carried out on a Bruker Autoflex III MALDI-TOF mass spectrometer (Bruker Daltonics, Bremen, Germany), which is equipped with a Smartbeam 2 Nd:YAG laser. LDI-MS images were constructed using the FlexImaging 2.1 software package. A total of 50 laser shots were measured per position. The step width between laser shots was 25 μm. The laser energy was optimized to ~ 61 μJ/pulse.

Statistical evaluation. Six areas of interest in the white pulp of the spleen tissue from a tumor-bearing mouse were analyzed using ImageJ software. Briefly, a 'freehand selection' function was employed to choose inside the white pulp areas and pixel frequencies were analyzed using a histogram function. Then, average pixel intensities

were calculated using the equation as below:

$$\text{Average pixel intensity} = \frac{\sum(\text{pixel intensity}) \times (\text{pixel number})}{\sum \text{pixel number}}$$

Only nonzero data containing pixels were counted and averaged for analysis following a reported method.[1] One-way ANOVA was performed in the statistical evaluation, and the *P* values were 0.26 (AuNP **1** and **2**), 8×10^{-6} (AuNP **2** and **3**), and 2×10^{-5} (AuNP **2** and **3**), respectively.

AuNP synthesis and characterization

AuNPs were synthesized by the Brust-Schiffrin two-phase method.[2] A Murray place exchange reaction followed to functionalize the NPs with different ligands[3]. The synthesis of ligands has been reported in previous work.[4-6]

The core sizes of the AuNPs used in this study were determined by TEM on a JEOL100S electron microscope (see panel a, b, and c in Figure S1). Dynamic light scattering (DLS) (see panel i, j, and k in Figure S1) and zeta-potential measurements of AuNPs (see panel l, m, and n in Figure S1) were obtained on a Malvern Nano Zetasizer (Nano series, Malvern Instruments Inc, USA) to evaluate quality and surface properties for the AuNPs. 2.5 μL of 2 μM solution of each AuNP was used for the LDI-MS characterization of surface ligands (Figure S2).[7]

Cell culture

TD cells[8,9] were cultured in Dulbecco's Modified Eagle's Medium/ Nutrient Mixture F-12 Ham (DMEM:F12, Sigma) supplemented with 25 mM of HEPES (Sigma), 14 mM of $NaHCO_3$, 2% bovine serum (Atlanta Biologicals, GA), 10 μg/mL of insulin (Sigma), 5

ng/mL of epidermal growth factor (EGF, Invitrogen, NY), 1% antibiotic/antimycotic solution (Gibco, NY), and 7.5 μg/mL of gentamicin (Gibco, NY).

Animal care

All animal experiments were conducted in accordance with the guidelines of Institutional Animal Care and Use Committee (IACUC) at University of Massachusetts-Amherst. Female Balb/c mice were purchased from Jackson Laboratory (Bar Harbor, ME). Food and water intake were assessed.

Intravenous administration of AuNPs in normal mice

After one week of acclimatization, 50 μL of each AuNP (2 μM) was administered intravenously to each mouse (Balb/c, 10 weeks), while 50 μL of Dulbecco's phosphate-buffered saline (DPBS) was administered intravenously in the control group. Mice were sacrificed and dissected 24 h after the intravenous administration of AuNPs. Mammary, brain, kidney, liver, spleen, lung, intestine, and heart were harvested and weighed for biodistribution and imaging.

Induction of mammary tumor and intravenous administration of AuNP mixture in tumor-induced mice

After one week of acclimatization, the mice (Balb/c, 3 weeks) were anesthetized intraperitoneally by Avertin (Acros, 200 mg/kg). Prior to cell transplantation, an analgesic agent, buprenorphine (0.05 mg/kg), was subcutaneously administrated. After removing the skin hair with a trimmer (Braintree Scientific, MA), an inverted Y-shaped incision was made along the ventral thoracic-inguinal region to expose the mammary fat pad.[10] Then, the region overlying the nipple and the mammary artery running between the 4th

and 5th mammary glands were separately cauterized. The mammary fat pads were gently removed using curved forceps.

TD cells ($5x10^4$ cells/50 μL) were transplanted into the cleared fat pad using a Hamilton syringe. The skin was closed by wound clips (9 mm Autoclips Applier, Braintree Scientific, MA) and ethicon suture (Braintree Scientific, MA). The wound clips were removed approximately 1 week after the surgical procedure. After a mammary tumor was grown, the mixture of AuNPs was administered intravenously to each mouse. After 24 h, the mice were humanely sacrificed by the inhalation of carbon dioxide followed cervical dislocation. Then, each organ sample was harvested and further analyzed. After cutting them into two parts, one half was digested overnight to analyze for total gold amount (ng) by ICP-MS, and another half was used for the LDI-MS imaging.

ICP-MS sample preparation and conditions

Each organ was digested overnight using a 3:1 (v/v) mixture of HNO_3 (68%) and H_2O_2 (30%). On the next day, ~0.5 mL of aqua regia was added, and then the sample was diluted to 10 mL with de-ionized water. (*Highly corrosive aqua regia must be added with extreme caution!*) A series of standard solutions (gold concentration: 20, 10, 5, 2, 1, 0.5, 0.2, 0 ppb) was prepared for each experiment. The ICP-MS analyses were performed on a Perkin-Elmer NexION 300X ICP mass spectrometer. ^{197}Au was measured under standard mode. Operating conditions are listed as below: nebulizer flow rate: 0.95-1 L/min; rf power: 1600 W; plasma Ar flow rate: 18 L/min; dwell time: 50 ms.

LDI-MS imaging tissue preparation

A Leica cryostat CM 3050 and 1850 were used to slice all tissues. The tissues were sliced under -20 °C, and the optimal tissue thickness was found to be 12 µm. Indium tin oxide (ITO) coated glass slides (Delta Technologies, Limited, Loveland, CO).

LDI-MS instrumentation and conditions

LDI-MS imaging was carried out on a Bruker Autoflex III MALDI-TOF mass spectrometer (Bruker Daltonics, Bremen, Germany), which is equipped with a Smartbeam 2 Nd:YAG laser. LDI-MS images were constructed using the FlexImaging 2.1 software package. LDI-MS operating conditions were as follows: ion source 1 = 19.00 kV, ion source 2 = 16.60 kV, lens voltage = 8.44 kV, reflector voltage = 20.00 kV, reflector voltage 2 = 9.69 kV, and positive reflectron mode in a mass range of 100−1200 Da. A total of 50 laser shots were measured per position. The step width between laser shots is 25 µm. The laser energy has been optimized to ~ 61 µJ/pulse.

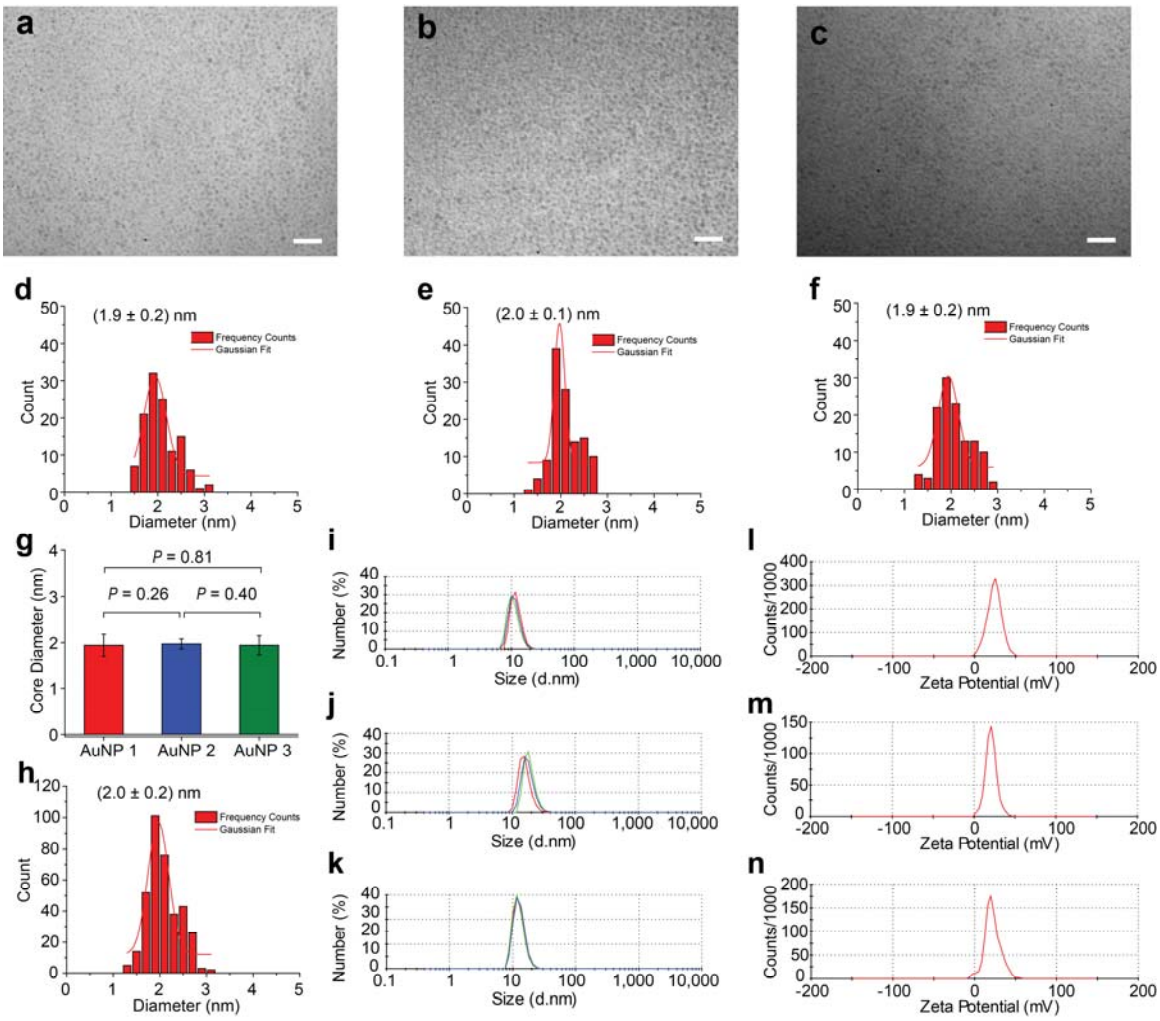

Figure S1. Characterization of AuNP 1-3. TEM images of the AuNPs after the Murray place-exchange reactions: **a**, AuNP **1**; **b**, AuNP **2**; and **c**, AuNP **3**. Core size distribution of each AuNP: **d**, AuNP **1**; **e**, AuNP **2**; and **f**, AuNP **3** (120 NPs were randomly selected). **g**, One-way ANOVA test indicates the same core size of these AuNPs (n = 120). **h**, Overall size distribution of three AuNPs (360 NPs). The hydrodynamic size of each AuNP was measured by dynamic light scattering (DLS): **i,** AuNP **1**; **j,** AuNP **2**; and **k,** AuNP **3**. Zeta-potential measurements of the AuNPs are shown in panel **l,** AuNP **1**; **m,** AuNP **2**; and **n,** AuNP **3**.

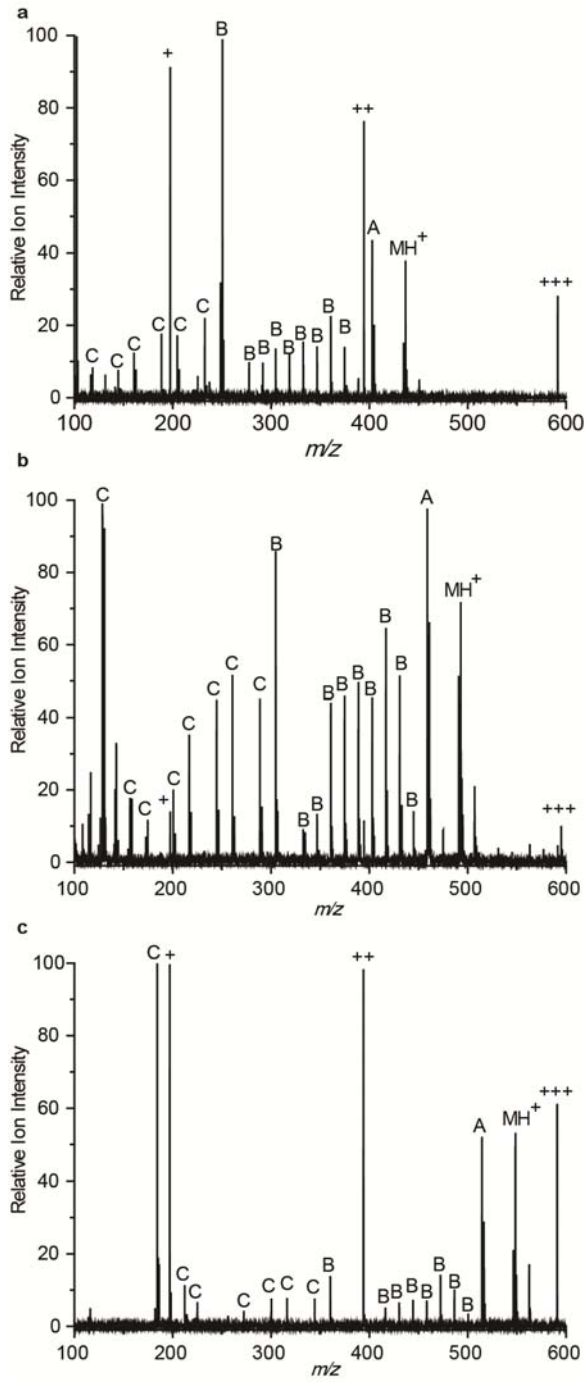

Figure S2. LDI-MS characterization of a, AuNP 1; b, AuNP 2, and c, AuNP 3. The LDI-MS results are consistent with previous research[5,7,11]. Symbol key: +, Au^+ (*m/z* 197); ++, Au_2^+ (*m/z* 394); +++, Au_3^+ (*m/z* 591); MH^+, the molecular ion corresponding to surface ligand; A, a fragment ion corresponding to a loss of

H_2S ([MH-H_2S]$^+$) from the intact ligand; B, ions corresponding to multiple losses of methylene groups from the alkane portion of the ligands; C, ions corresponding to multiple losses of ethylene glycol groups from the ligands.

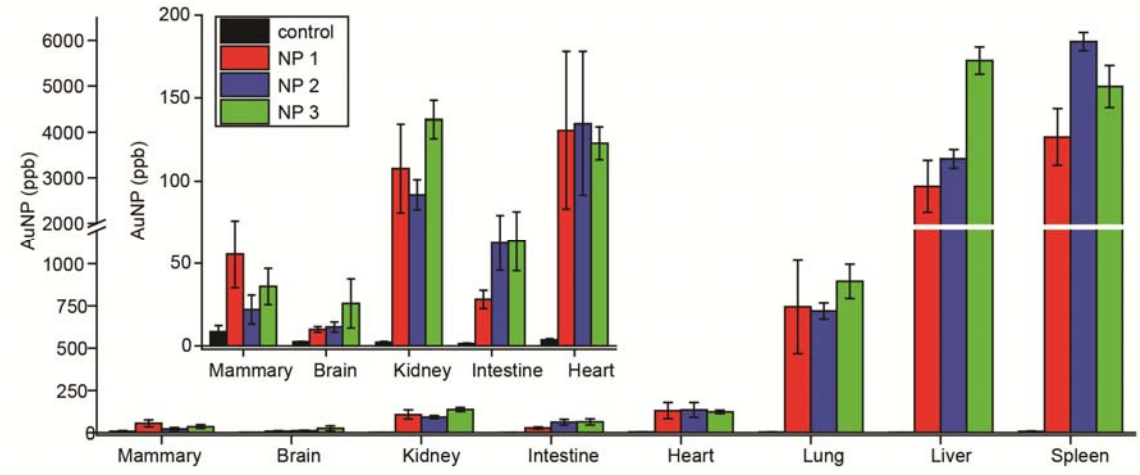

Figure S3. AuNP amounts in different organs as determined by ICP-MS. The AuNP concentrations were calculated by the gold amount (ng) divided by organ weight (g) (± standard error of the mean). (control group: n = 3, experimental group: n = 4).

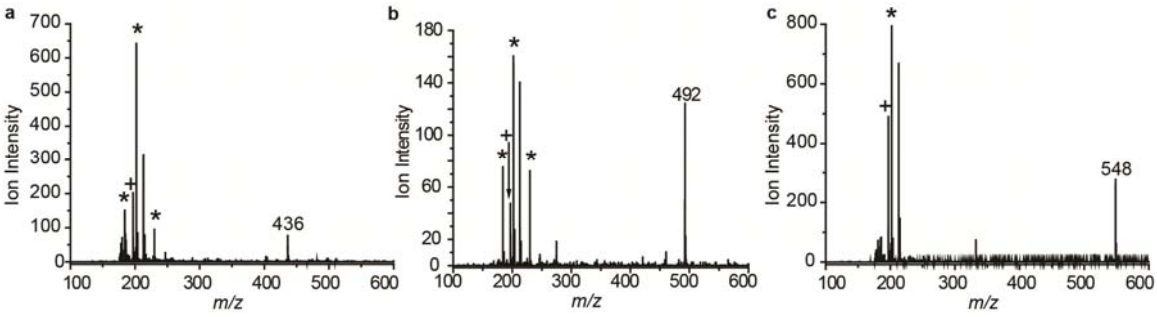

Figure S4. Representative LDI mass spectra of AuNPs in mouse spleen. a, AuNP **1** (molecular ion *m/z* = 436). **b**, AuNP **2** (molecular ion *m/z* = 492). **c**, AuNP **3** (molecular ion *m/z* = 548). Other ions in the spectra correspond to fragments of the phosphatidylcholine head groups (*m/z* 184, 202, and 230), which are indicated with *, and Au^+ (*m/z* 197), which is indicated by a +.

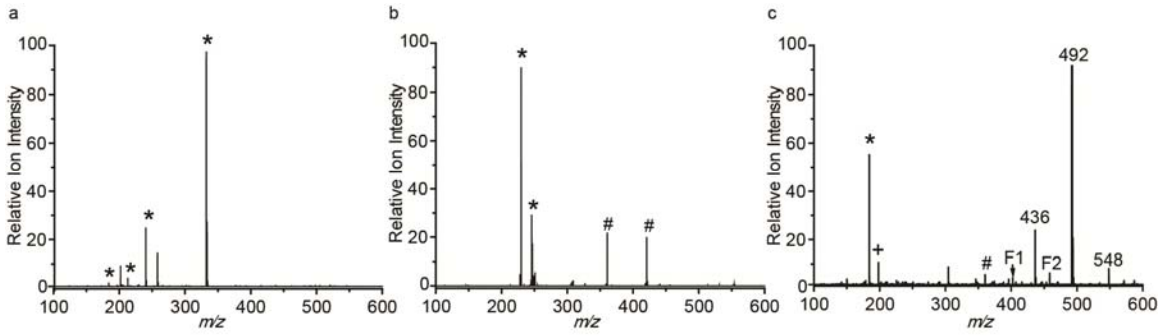

Figure S5. LDI-MS on spleen tissue from mouse injected with DPBS buffer. Control experiments to confirm that the "mass barcodes" of AuNPs are only observed when the ligands are attached on the gold cores. (a) Typical LDI mass spectrum of spleen tissues from a mouse that was not injected with AuNPs. (b) Typical LDI mass spectrum of a tissue slice from a non-injected mouse that was spiked with free ligands (1 μL of 5 μM ligand mixure solution). (c) Example LDI mass spectrum of a spleen slice from a non-injected mouse that was spiked with 1 μL of a 50 nM mixture of AuNP **1**, AuNP **2**, and AuNP **3**. Symbol key: *, ions from phosphatidylcholine head groups; +, gold ions; #, interference ions from the ITO glass slide; F1 and F2, fragment ions corresponding to a loss of H_2S ($[MH\text{-}H_2S]^+$) from molecular ions of ligands on **AuNP 1** and **2**, respectively.

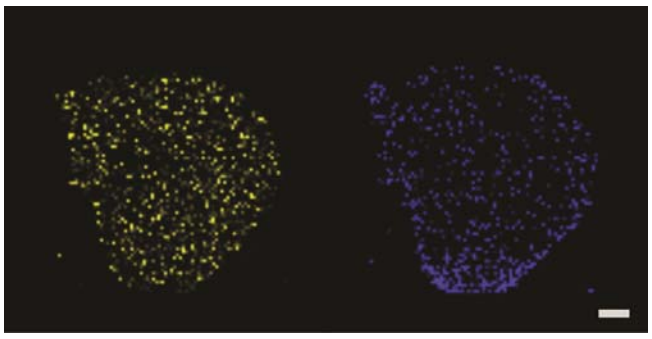

Figure S6. LDI-MS images of AuNP 2 in mouse liver tissue. Left: LDI-MS image of gold ions; right: LDI-MS image of ligand ion from AuNP **2** (*m/z* = 492) (scale bar represents 1 mm).

Sensitivity of LDI-MS imaging

We have evaluated the sensitivity of this new imaging technique using equation as below:

$$n_i = \frac{V \times d}{M_{Au}} = \frac{\pi(\frac{D}{2})^2 \times h \times c_{Au} \times d_{Tissue}}{M_{Au}} \quad (1)$$

The amount of each AuNP (n_i) per laser shot has been calculated using the volume of the sample for each LDI-MS measurement location (V), the density of the gold in the tissue (d) and the amount of gold in each AuNP (M_{Au}). We measured the size of the laser burn (D) to be (45 ± 6) μm on the tissue after the LDI-MS imaging experiment by optical microscopy (Figure S6). The thickness of each tissue (h) is 12 μm, and thus the volume of the tissue sample for each LDI-MS measurement location is 19 pL. ICP-MS has been used to detect the concentration of gold in tissues (c_{Au}) (Figure S3) and M_{Au}. The c_{Au} for AuNP **1**, **2**, and **3** used in the imaging experiments in Figure 2 are 5.34, 5.95, and 5.72 μg/g, respectively. We assume the density of the tissue (d_{Tissue}) is 1.08 g/cm^3.[12] Finally, as for sensitivity in tissues, the LDI-MS imaging technique has successfully detected 1.1, 1.3, and 1.2 attomol of AuNP **1**, **2**, and **3** used in this study, respectively.

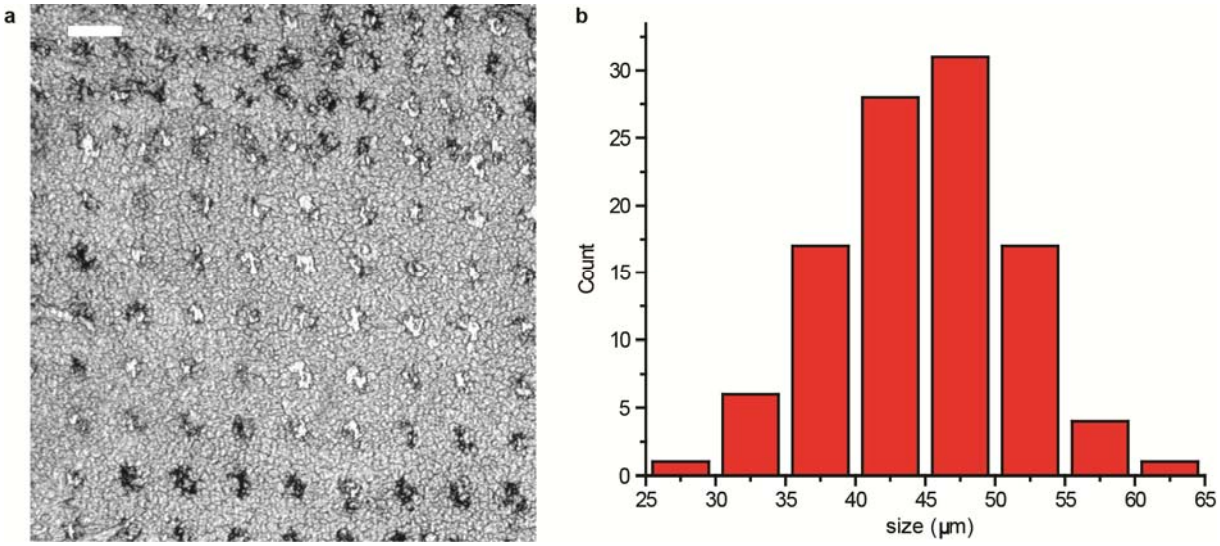

Figure S7. Sensitivity determination of the LDI-MS imaging technique. a, Optical microscopy image of the laser burns on a 12-µm thickness splenic tissue. Laser stepwidth: 100 µm. Scale bar represents 100 µm. **b**, Laser burn size distribution (100 measurements), size of the laser burns: (45 ± 6) µm.

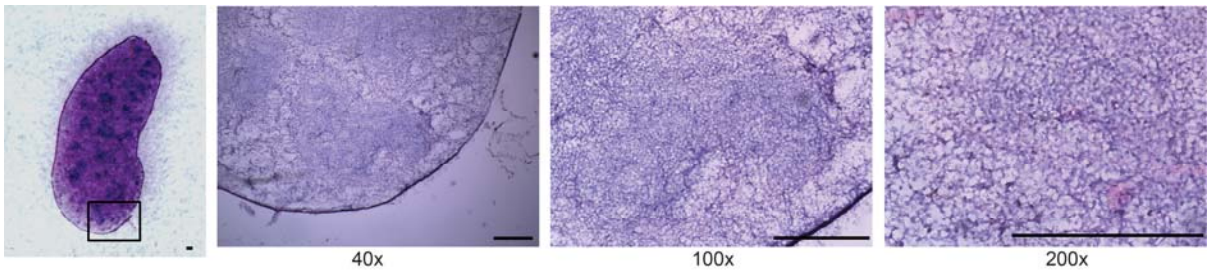

Figure S8. H&E staining images of the splenic tissue. (Scale bar = 200 µm)

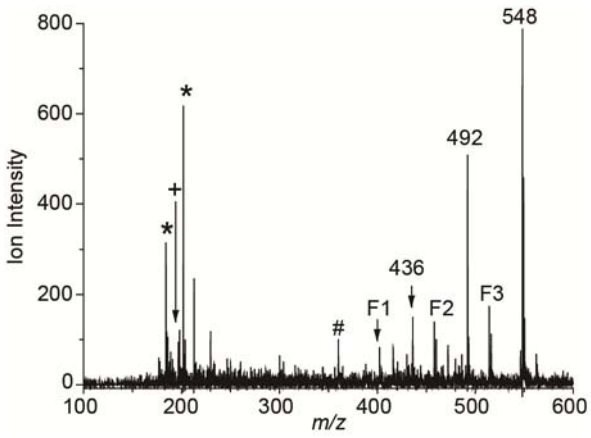

Figure S9. Representative mass spectrum of the red pulp region of the spleen. Symbol key: *, ions from phosphatidylcholine head groups; +, gold ions; #, interference ions from the ITO glass slide; F1, F2, and F3, fragment ions corresponding to a loss of H_2S ($[MH\text{-}H_2S]^+$) from molecular ions of ligands on **AuNP 1**, **2**, and **3**, respectively.[7]

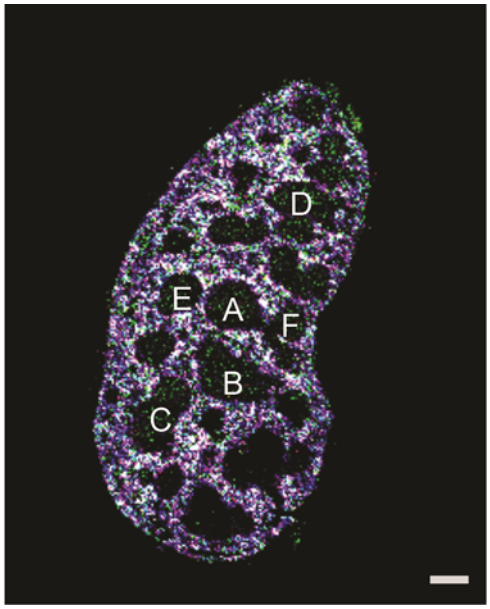

Figure S10. White pulp regions selected for the statistical evaluation. (Scale bar = 500 μm).

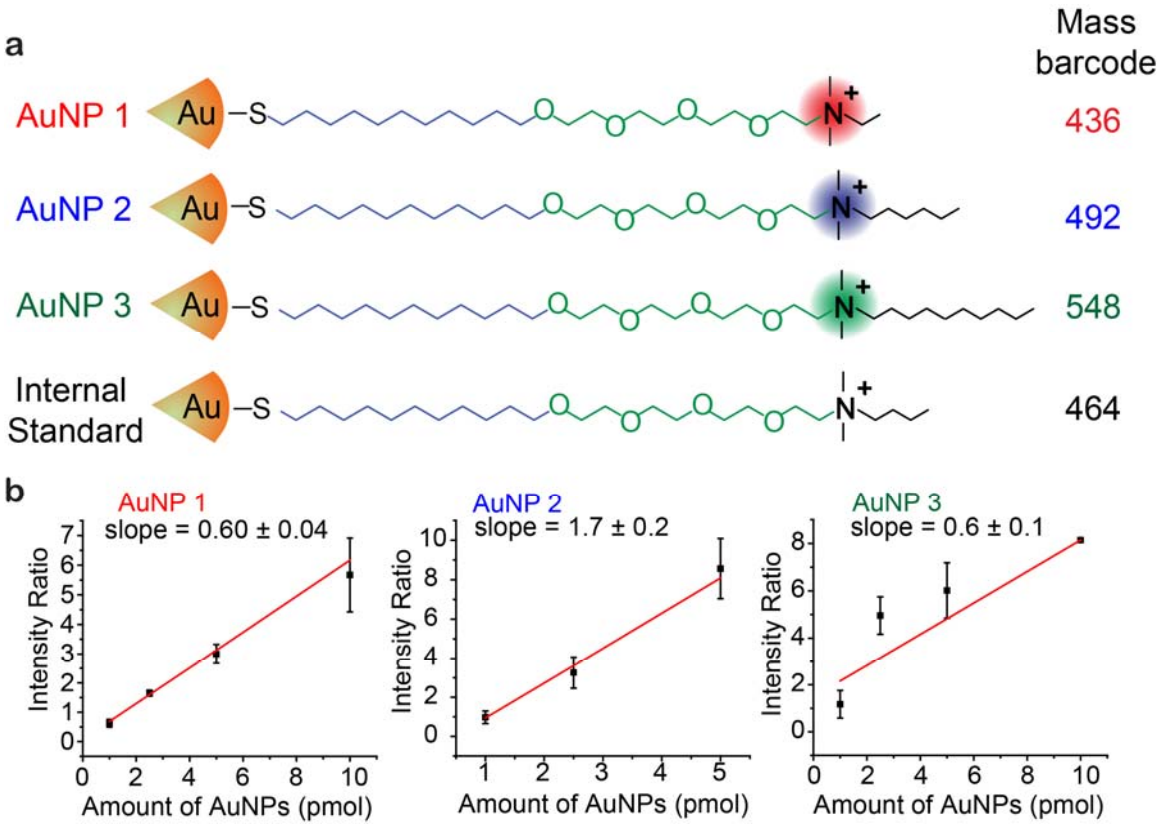

Figure S11. Relative ionization efficiencies of AuNP 1-3. (a) A constant concentration of an internal standard AuNP (I.S.) was mixed with different concentrations of AuNP **1-3** in cell lysates and then analyzed by LDI-MS. (b) The LDI-MS intensity ratios between AuNP **1-3** and I.S. were then plotted against the concentrations of AuNP **1-3**. The resulting slopes for each NP provide a relative measure of their ionization efficiency because the same I.S. AuNP is used in each case.

Author Contributions

B.Y., V.M.R., and R.W.V. conceived and designed the experiments. B.Y., S.T.K., C.S.K., K.S., D.F.M., Y.X., Y.J., A.L.R., and F.S.A. performed the experiments. B.Y. developed the imaging technique, S.T.K., A.L.R., C.S.K., and K.S. did the animal experiments, D.F.M. synthesized the NPs, B.Y., Y.X., Y.J., and F.S.A. quantified the gold amounts in tissues. All authors analyzed and discussed the data. The manuscript was prepared by B.Y., R.W.V., V.M.R., C.S.K, S.T.K., and K.S. All authors have given approval to the final version of the manuscript.

References:

1. Kim, C. S.; Qi, W.; Zhang, J.; Kwon, Y. J.; Chen, Z. *J. Biomed. Opt*. **2013**, *18*, 030504.

2. Brust, M.; Walker, M.; Bethell, D.; Schiffrin, D. J.; Whyman, R. *J. Chem. Soc. Chem. Comm.* **1994**, 801.

3. Templeton, A. C.; Wuelfing, M. P.; Murray, R. W. *Acc. Chem. Res.* **2000**, *33*, 27.

4. Miranda, O. R.; Li, X. N.; Garcia-Gonzalez, L.; Zhu, Z. J.; Yan, B.; Bunz, U. H. F.; Rotello, V. M. *J. Am. Chem. Soc.* **2011**, *133*, 9650.

5. Zhu, Z. J.; Ghosh, P. S.; Miranda, O. R.; Vachet, R. W.; Rotello, V. M. *J. Am. Chem. Soc.* **2008**, *130*, 14139.

6. You, C. C.; Miranda, O. R.; Gider, B.; Ghosh, P. S.; Kim, I. B.; Erdogan, B.; Krovi, S. A.; Bunz, U. H. F.; Rotello, V. M. *Nat. Nanotechnol.* **2007**, *2*, 318.

7. Yan, B.; Zhu, Z. J.; Miranda, O. R.; Chompoosor, A.; Rotello, V. M.; Vachet, R. W. *Anal. Bioanal. Chem.* **2010**, *396*, 1025.

8. Bajaj, A.; Miranda, O. R.; Kim, I. B.; Phillips, R. L.; Jerry, D. J.; Bunz, U. H.; Rotello, V. M. *Proc. Natl. Acad. Sci. USA.* **2009**, *106*, 10912.

9. Blackburn, A. C.; McLary, S. C.; Naeem, R.; Luszcz, J.; Stockton, D. W.; Donehower, L. A.; Mohammed, M.; Mailhes, J. B.; Soferr, T.; Naber, S. P.; Otis, C. N.; Jerry, D. J. *Cancer Res.* **2004**, *64*, 5140.

10. Dunphy, K. A.; Tao, L.; Jerry, D. J. *J. Vis. Exp.* **2010**, *40*, e1849.

11. Creran, B.; Yan, B.; Moyano, D. F.; Gilbert, M. M.; Vachet, R. W.; Rotello, V. M. *Chem. Commun.* **2012**, *48*, 4543.

12. Steinman, R. M.; Witmer, M.D. *Proc. Natl Acad. Sci. USA.* **1978**, *75*, 5132.